Supporting Information

Conjugated Conductive Polymer Coating Towards Robust Micro-Si Anode for Lithium Storage

Song Chao, Jiecheng Huang and Zhiyu Wang

E-mail: zywang@dlut.edu.cn

Experimental Section

Chemicals and materials.

Micrometer-sized Si powder (1−3 μm in size) were purchased from Aladdin. The polyacrylonitrile (PAN, Mw 150,000), Polyacrylic acid-Li (PAA-Li, Mw 450,000), N, N-dimethylformamide (DMF, AR) and Super P (Vulcan XC72) were purchased from Sigma-Aldrich. The electrolyte (LB-008) was purchased from DodoChem.

Preparation of μSi@C

Commercial micrometer-sized Si powder (1−3 μm in size, 0.3 g) was uniformly dispersed in ethanol solution (200 mL) of PAN (0.9 g) under ultrasonic for 2 h. Afterward, the solution was heated at 100℃ overnight to remove ethanol. The obtained product was annealed at 800 ℃ at a ramp rate of 5 ℃ min^{-1} in Ar flow for 3 h, yielding μSi@C.

Preparation of μSi@C@CP

A mixture of μSi@C (140 mg) and PAN (60 mg) was uniformly dispersed in DMF (800 μL) under stirring and ultrasonic for 0.5 h. The obtained slurry was evenly cast on Cu foil, followed by drying at 100 ℃ for 12 h to remove DMF. The obtained product was annealed at 300℃ at a ramp rate of 5 ℃ min^{-1} in Ar flow for 2 h, yielding μSi@C@CP anode.

Material characterization

Scanning electron microscopy (SEM, JEOL JSM-7900F) with an energy dispersive spectrometer (EDS) and transmission electron microscope (TEM, Tecnai G2 F30 S-Twin) was employed to observe the morphology of the materials. X-ray diffraction (XRD, Bruker D8 Advance, Cu Kα), X-ray photoelectron spectroscopy (XPS, Thermo ESCALAB 250), Thermogravimetric analyzer (METTLER TOLEDO TGA/DSC3+) and Fourier transform infrared spectrometer (FTIR, NicoletIS50) were used to investigate the chemical composition of the samples. The N_2 adsorption-desorption measurement of the samples were performed on a Micrometrics ASAP 2020 Surface Area and Porosity Analyzer.

Battery test

The battery tests were conducted using CR2016 coin cells with Li foil as the counter and reference electrode at 30 ºC. The μSi@C@CP anode was directly used as working electrode. For μSi@C and μSi, the working electrode consists of an active material, carbon black (Super P) and PAA-Li binder in a weight ratio of 7:1.5:1.5. The mass loading was controlled to 1.0 to 1.2 mg cm^{-2}. The electrolyte used is 1.0 M $LiPF_6$ in a 50:50 (w/w) mixture of ethylene carbonate (EC) and diethyl carbonate (DEC) with 10 wt.% fluoroethylene carbonate (FEC). Cell assembly was carried out in an Ar-filled glovebox with the concentration of moisture and oxygen below 1.0 ppm.

The galvanostatic charge/discharge tests were performed using a LAND CT2001A battery tester at different current densities within a cut-off voltage window of 0.01–1.5 V (vs. Li/Li^+). The specific capacities were calculated based on the total mass of the active materials. Cyclic voltammetry (CV) studies were conducted using an IVIUM Vertex.C. electrochemical workstation between 0.01-1.5 V (vs. Li/Li^+) at different scan rates. The electrochemical impedance spectrum (EIS) were recorded in a frequency range of 100 kHz – 0.01 Hz with 5 mV amplitude. The cells were rested for 10 min to minimize the polarization before each EIS measurement.

***In-situ* XRD tests**

In-situ XRD analysis were performed using μSi@C@CP anode against Li foil. The electrolyte is 1.0 M $LiPF_6$ in a 50:50 (w/w) mixture of EC and DEC with 10 wt.% FEC. *In-situ* XRD patterns were recorded using an X-ray diffractometer with a 2D detector (Bruker D8 DISCOVER) on a cell module with Be window. The XRD patterns were collected per 600 s in a 2θ range of 27 to 30°. Meanwhile, the discharge-charge tests of

the half cells were conducted at a current density of 0.1 A g^{-1} between 0.01–1.5 V (*vs.* Li/Li^+).

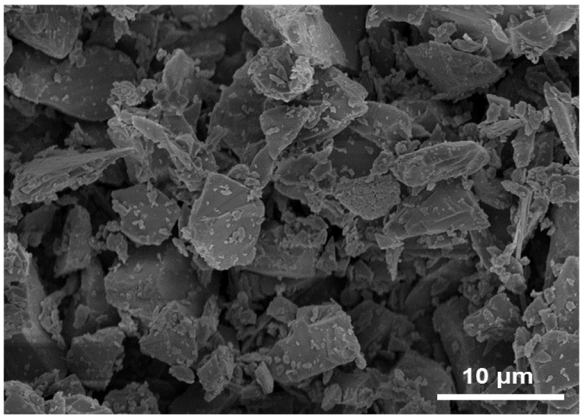

Fig. S1 SEM image of commercial μSi.

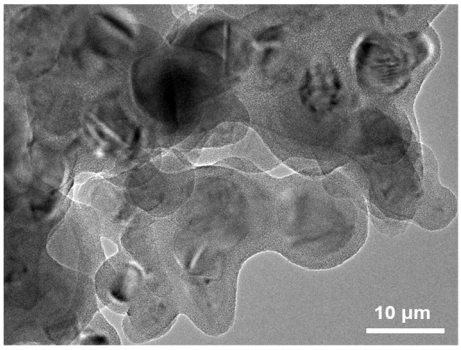

Fig. S2 TEM image showing the presence of continuous CP coating bridging adjacent μSi@C particles.

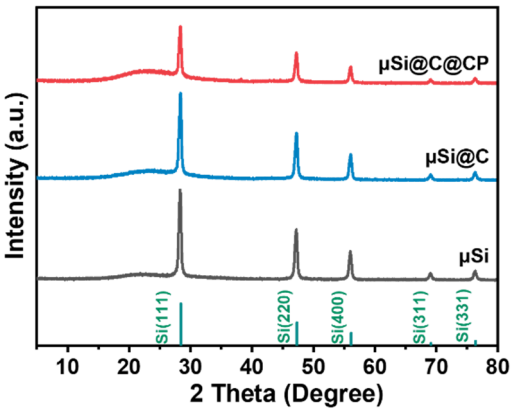

Fig. S3 XRD patterns of μSi@C@CP, μSi@C and μSi

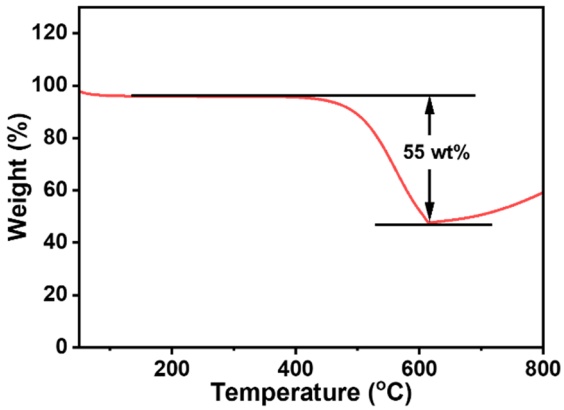

Fig. S4 TGA curve of μSi@C@CP in air at a ramp rate of 10 °C min^{-1}.

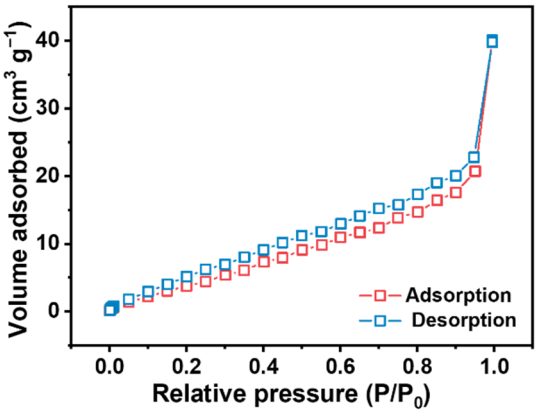

Fig. S5 N_2 adsorption-desorption isotherms of μSi@C@CP.

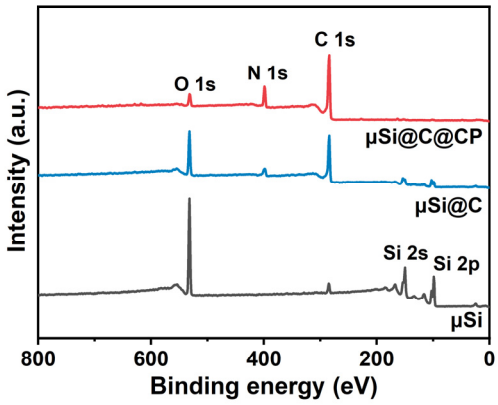

Fig. S6 XPS full-scan survey of μSi@C@CP, μSi@C and μSi.

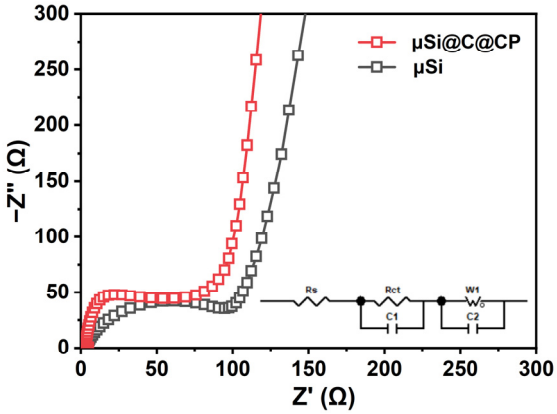

Fig. S7 EIS spectra of μSi@C@CP and μSi.

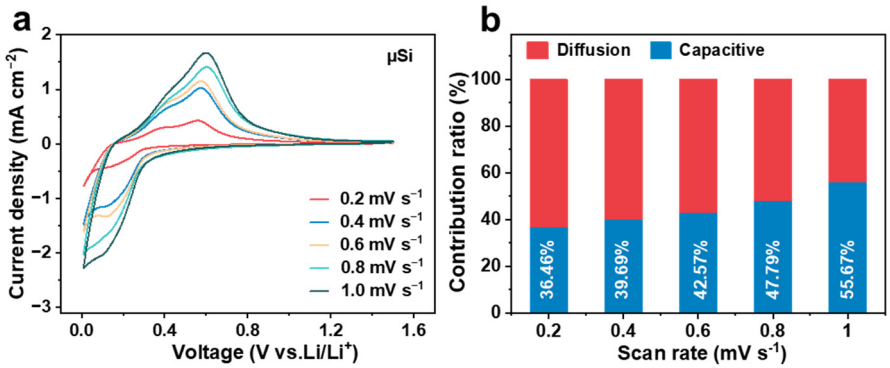

Fig. S8 (a) CV curves of μSi anode at various scan rates. (b) The contribution ratios of diffusion-controlled and capacitance processes for Li storage in μSi anode.

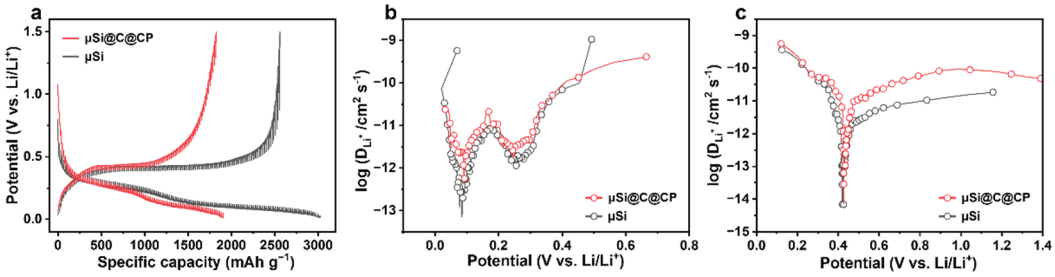

Fig. S9 (a) GITT curves of μSi@C@CP and μSi anode. Corresponding variation of D_{Li+} during (b) discharge and (c) charge process of μSi@C@CP and μSi anode.